

## Selective Shortening of Single-Crystalline Gold Nanorods by Mild Oxidation

Chia-Kuang Tsung,<sup>†,‡</sup> Xiaoshan Kou,<sup>‡</sup> Qihui Shi,<sup>†</sup> Jinping Zhang,<sup>§</sup> Man Hau Yeung,<sup>‡</sup>  
Jianfang Wang,<sup>\*,‡</sup> and Galen D. Stucky<sup>\*,†,§</sup>

Department of Chemistry and Biochemistry and Materials Department, University of California, Santa Barbara, California 93106, and Department of Physics, the Chinese University of Hong Kong, Shatin, Hong Kong, P. R. China

Received January 20, 2006; E-mail: stucky@chem.ucsb.edu; jfwang@phy.cuhk.edu.hk

Gold nanorods (NRs) have many potential applications because their longitudinal plasmon band (LPB) is highly sensitive to their aspect ratios.<sup>1,2</sup> Methods that have been developed for preparing Au NRs include electrochemical deposition,<sup>3</sup> photochemistry,<sup>4</sup> and seed-mediated synthesis.<sup>5,6</sup> The introduction of Ag<sup>+</sup> in growth solutions significantly improves the yield of Au NRs.<sup>3,4,6</sup>

The aspect ratio of Au NRs can be controlled not only during synthesis but also by resizing after growth. Size reduction of Au NRs has been demonstrated with thermal/laser heating<sup>7</sup> and cyanide/Au(III) dissolution.<sup>8</sup> Here we report a simple approach for the selective shortening of single-crystalline Au NRs by mild oxidation with environmentally benign oxygen. The oxidation rate is controlled by temperature and acid concentration. Compared with previous resizing methods, this approach provides better controllability and can be used to produce single-crystalline Au NRs of any desired aspect ratio with narrow size distributions within the limit of that possessed by the starting Au NRs.

The starting Au NRs were prepared using the silver ion-assisted seed-mediated method<sup>6</sup> [Supporting Information (SI)]. For oxidation, the as-synthesized Au NR solution was mixed with certain amounts of 1 M HCl and then maintained at certain temperatures with continuous stirring and bubbling of O<sub>2</sub>. Real-time UV–visible extinction spectra were monitored with a fiber-optic spectrometer. Both low-magnification and high-resolution (HR) transmission electron microscopy (TEM) images were taken on Au NR samples obtained after varying oxidation time.

Figure 1a shows the extinction spectra acquired at varying stages of Au NR oxidation. Starting Au NRs exhibit two extinction peaks, corresponding to the transverse plasmon band (TPB) and LPB. The LPB blue-shifts and decreases in intensity with oxidation, while the TPB stays at 520 nm and decreases in intensity. Upon further oxidation, the LPB becomes a shoulder of the TPB and finally disappears, suggesting the conversion of NRs into nanospheres. Au nanospheres are eventually completely oxidized, as indicated by the disappearance of the extinction peak at 520 nm. Portions of Au NR solutions can be taken out after varying oxidation time and rapidly cooled to room temperature to stop oxidation, producing Au NRs that exhibit varying longitudinal plasmon wavelengths (LPWs) with distinct colors (SI Figure S1).

TEM imaging shows that starting Au NRs exhibit a narrow size distribution (Figure 1b). Au NRs decrease in length with oxidation (Figure 1c and SI Figure S2) and then become nanospheres (Figure 1d). Size measurements of 200–500 Au NRs per sample reveal that the length decreases with decreasing LPW, and that the diameter stays almost constant (Figure 1e), suggesting that oxidation starts at the ends of the Au NRs. This anisotropic reaction has also been

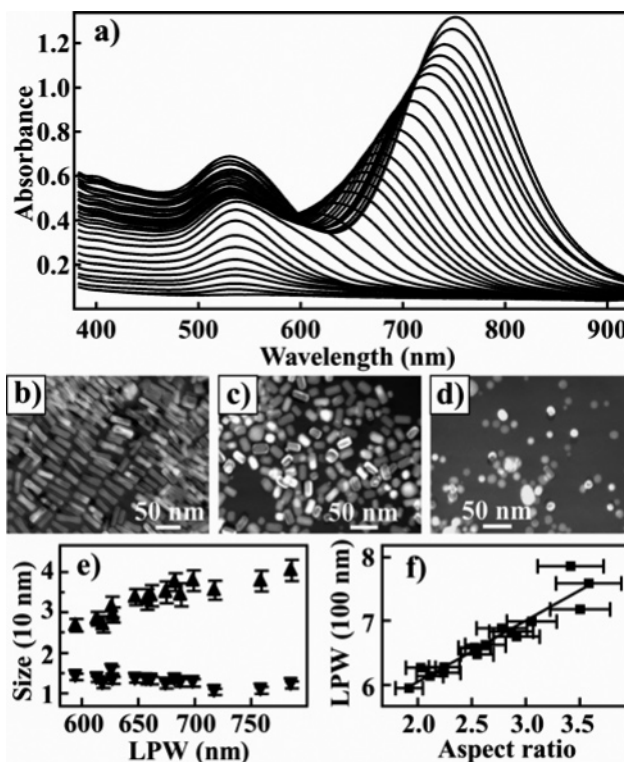


**Figure 1.** Oxidation of Au NRs. (a) UV–visible spectra acquired every 1 min. The solution was a mixture of as-synthesized Au NR solution and 1 M HCl at a volume ratio of 1.0 and was kept at 70 °C. (b) TEM image of as-synthesized Au NRs (LPW = 785 nm). (c) TEM image of shortened Au NRs (LPW = 595 nm). (d) TEM image of spherical Au nanoparticles obtained from Au NR oxidation. (e) The changes of Au NR lengths ( $\blacktriangle$ ) and diameters ( $\blacktriangledown$ ) versus LPWs. (f) The relationship between LPWs and aspect ratios. The line is a linear fit. Error bars in (e) and (f) represent standard deviations.

observed previously in dissolving nonspherical Au nanoparticles with cyanide and Au(III).<sup>8</sup> We have determined the aspect ratios of Au NRs with different LPWs (Figure 1f). The LPW decreases approximately linearly with the aspect ratio, which is in agreement with previous results.<sup>1–3,6</sup> Moreover, the standard deviations in lengths, diameters, and aspect ratios of shortened Au NRs are comparable to or even smaller than those of starting NRs (SI Figure S3), indicating a clear advantage of this mild oxidation approach for the preparation of Au NRs of varying aspect ratios.

The oxidation rate of Au NRs is controlled by the acid concentration (Figure 2a) and reaction temperature (Figure 2b). The blue-shift of the LPB appears linear with time, and the slope can be used to characterize the oxidation rate. At 70 °C, the oxidation rate of Au NRs in as-synthesized solutions with a pH around 3 is 0.49 nm/min. It increases to 4.3 and 5.9 nm/min, respectively, when

<sup>†</sup> Department of Chemistry and Biochemistry, UCSB.

<sup>‡</sup> Chinese University of Hong Kong.

<sup>§</sup> Materials Department, UCSB.

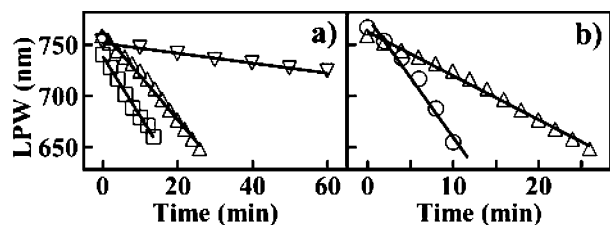


**Figure 2.** Variation of the oxidation rate of Au NRs by control of (a) the acid concentration and (b) temperature.  $\nabla$ : as-synthesized Au NR solution at 70 °C;  $\triangle$ : mixture of 1 M HCl and NR solution at a volume ratio of 0.4 at 70 °C;  $\square$ : mixture of 1 M HCl and NR solution at a volume ratio of 1.0 at 70 °C;  $\circ$ : mixture of 1 M HCl and NR solution at a volume ratio of 0.4 at 90 °C. The oxidation rates are 0.49(3), 4.3(1), 5.9(2), and 11.7(5) nm/min for  $\nabla$ ,  $\triangle$ ,  $\square$ , and  $\circ$ , respectively. The numbers in the parentheses are the uncertainties in the last digits.

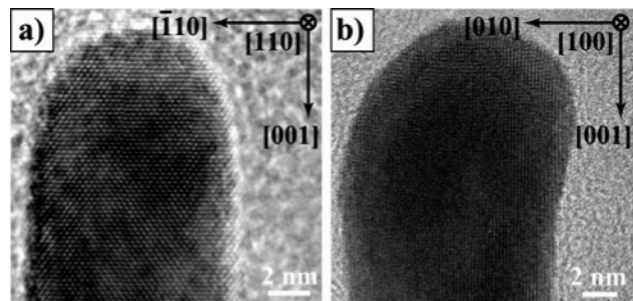


**Figure 3.** HRTEM images of Au NRs oriented in (a) the [110] and (b) the [100] direction.

the acid concentration is increased by adding 1 M HCl to NR solution at a volume ratio of 0.4 and 1.0. The oxidation rate can also be enhanced by increasing the reaction temperature. For the mixtures of 1 M HCl and Au NR solution at a volume ratio of 0.4, the oxidation rate is increased from 4.3 to 11.7 nm/min when the temperature is increased from 70 to 90 °C.

HRTEM imaging has been carried out to investigate the relationship between the crystal structure and oxidation. Au and Ag NRs often exhibit twinned crystal structures.<sup>9,10</sup> It has been found that twinned Ag nanoparticles can be etched by O<sub>2</sub>, leaving only single-crystalline ones to grow larger.<sup>11</sup> In our experiments, starting Au NRs are observed to be single crystalline without twin planes. They stay single crystalline during oxidation (Figure 3 and SI Figure S4), suggesting that twinning is not involved in the oxidation process. Out of 30 NRs that exhibit the lattice structure from TEM imaging, 27 are [110] oriented and 3 are [100] oriented. This observation of Au NRs with a dominating [110] orientation is in agreement with previous results on Au NRs synthesized in the presence of silver ions.<sup>12</sup>

Control experiments have been performed to investigate the oxidation reaction of the Au NRs. First, O<sub>2</sub> is required for the complete dissolution of Au NRs. Au NR solutions kept at 50–90 °C without supplying O<sub>2</sub> exhibited only a blue-shift of 50–100 nm in the LPB, due to O<sub>2</sub> dissolved in NR solutions. Second, a high concentration of cetyltrimethylammonium bromide (CTAB) is required for NR oxidation. Au NRs washed by centrifugation and dispersed into water showed no blue-shift of the LPB. NRs that were washed, dispersed into 0.1 M cetyltrimethylammonium chloride, and mixed with 1 vol equiv of 1 M HCl first exhibited a blue-shift of the LPB at a rate of <0.05 nm/min at 90 °C and then stopped at ~700 nm. However, Au NRs washed and dispersed in 0.1 M CTAB exhibited the same oxidation behavior as as-

synthesized Au NR solutions, suggesting the blue-shift of the LPB is not due to remaining Au salt and oxidized ascorbic acid.<sup>13</sup> Third, as-synthesized Au NR solutions mixed with 35 wt % H<sub>2</sub>O<sub>2</sub> first become clear rapidly and then turn yellow after ~5 min. Last, oxidation experiments were carried out on Au NRs synthesized without the use of Ag<sup>+</sup>.<sup>5</sup> However, the low yield of Au NRs precluded the characterization of the oxidation process by extinction measurements. These control experiments suggest that O<sub>2</sub> is the oxidizing agent of Au NRs and that Br<sup>-</sup> acts as the complexing agent. O<sub>2</sub> oxidizes Au NRs into colorless AuBr<sub>2</sub><sup>-</sup>, but not into yellow AuBr<sub>4</sub><sup>3-</sup> (SI). An increase in the acid concentration enhances the oxidation rate of Au NRs because the addition of H<sup>+</sup> increases the reduction potential of the half-reaction involving O<sub>2</sub>.

In summary, we have demonstrated a method for continuous selective shortening of Au NRs by mild oxidation with O<sub>2</sub>. This shortening method can be used to produce Au NRs of any desired aspect ratio with narrow size distributions within the limit of that possessed by starting NRs. In addition, the anisotropic oxidation behavior observed here might provide some clues to the growth mechanism of Au NRs, as both growth and shortening reactions occur preferentially at the ends of single-crystalline NRs.

**Acknowledgment.** This research was supported in part by the Institute for Collaborative Biotechnologies through Grant DAAD19-03-D-0004 from U.S.A. Army Research Office and by the National Science Foundation, Grant no. DMR 02-33728. J.F.W. is grateful to CUHK for start-up funding support.

**Supporting Information Available:** Digital pictures, TEM images, and size distributions of shortened Au NRs. This material is available free of charge via the Internet at <http://pubs.acs.org>.

## References

- (1) (a) Pérez-Juste, J.; Pastoriza-Santos, I.; Liz-Marzán, L. M.; Mulvaney, P. *Coord. Chem. Rev.* **2005**, *249*, 1870–1901. (b) Murphy, C. J.; Sau, T. K.; Gole, A. M.; Orendorff, C. J.; Gao, J. X.; Gou, L. F.; Hunyadi, S. E.; Li, T. *J. Phys. Chem. B* **2005**, *109*, 13857–13870.
- (2) (a) Link, S.; Mohamed, M. B.; El-Sayed, M. A. *J. Phys. Chem. B* **1999**, *103*, 3073–3077. (b) Yan, B. H.; Yang, Y.; Wang, Y. C. *J. Phys. Chem. B* **2003**, *107*, 9159.
- (3) (a) van der Zande, B. M. I.; Böhmer, M. R.; Fokkink, L. G. J.; Schönenberger, C. *J. Phys. Chem. B* **1997**, *101*, 852–854. (b) Yu, Y.-Y.; Chang, S.-S.; Lee, C.-L.; Wang, C. R. C. *J. Phys. Chem. B* **1997**, *101*, 6661–6664.
- (4) (a) Kim, F.; Song, J. H.; Yang, P. D. *J. Am. Chem. Soc.* **2002**, *124*, 14316–14317. (b) Niidome, Y.; Nishioka, K.; Kawasaki, H.; Yamada, S. *Chem. Commun.* **2003**, 2376–2377.
- (5) (a) Jana, N. R.; Gearheart, L.; Murphy, C. J. *Adv. Mater.* **2001**, *13*, 1389–1393. (b) Jana, N. R.; Gearheart, L.; Murphy, C. J. *J. Phys. Chem. B* **2001**, *105*, 4065–4067. (c) Busbee, B. D.; Obare, S. O.; Murphy, C. J. *Adv. Mater.* **2003**, *15*, 414–416.
- (6) (a) Nikoobakht, B.; El-Sayed, M. A. *Chem. Mater.* **2003**, *15*, 1957–1962. (b) Sau, T. K.; Murphy, C. J. *Langmuir* **2004**, *20*, 6414–6420. (c) Orendorff, C. J.; Murphy, C. J. *J. Phys. Chem. B* **2006**, *110*, 3990–3994.
- (7) (a) Mohamed, M. B.; Ismail, K. Z.; Link, S.; El-Sayed, M. A. *J. Phys. Chem. B* **1998**, *102*, 9370–9374. (b) Link, S.; Burda, C.; Nikoobakht, B.; El-Sayed, M. A. *J. Phys. Chem. B* **2000**, *104*, 6152–6163.
- (8) (a) Jana, N. R.; Gearheart, L.; Obare, S. O.; Murphy, C. J. *Langmuir* **2002**, *18*, 922–927. (b) Rodríguez-Fernández, J.; Pérez-Juste, J.; Mulvaney, P.; Liz-Marzán, L. M. *J. Phys. Chem. B* **2005**, *109*, 14257–14261.
- (9) (a) Gai, P. L.; Harmer, M. A. *Nano Lett.* **2002**, *2*, 771–774. (b) Johnson, C. J.; Dujardin, E.; Davis, S. A.; Murphy, C. J.; Mann, S. *J. Mater. Chem.* **2002**, *12*, 1765–1770.
- (10) (a) Sun, Y. G.; Mayers, B.; Herricks, T.; Xia, Y. N. *Nano Lett.* **2003**, *3*, 955–960. (b) Ni, C. Y.; Hassan, P. A.; Kaler, E. W. *Langmuir* **2005**, *21*, 3334–3337.
- (11) Wiley, B.; Herricks, T.; Sun, Y. G.; Xia, Y. N. *Nano Lett.* **2004**, *4*, 1733–1739.
- (12) (a) Wang, Z. L.; Mohamed, M. B.; Link, S.; El-Sayed, M. A. *Surf. Sci.* **1999**, *440*, L809–L814. (b) Liu, M. Z.; Guyot-Sionnest, P. *J. Phys. Chem. B* **2005**, *109*, 22192–22200.
- (13) Gou, L. F.; Murphy, C. J. *Chem. Mater.* **2005**, *17*, 3668–3672.

JA060447T